Spin-State Isomerism in Crystalline [Fe^{III}(TPP)(OSO_2CF_3)]

Jorge A. González and Lon J. Wilson*

Department of Chemistry and Laboratory for Biochemical and Genetic Engineering, Rice University, P.O. Box 1892, Houston, Texas 77251

Received June 29, 1993®

The unsolvated porphyrin compound (trifluoromethanesulfonato)(*meso*-tetraphenylporphinato)iron(III), [Fe^{III}(TPP)(OSO_2CF_3)], has been structurally characterized by single-crystal X-ray diffraction in a monoclinic phase at 298 K and in a triclinic phase at 293 K and 188 K. While only one type of molecular site is found in the monoclinic phase, the temperature-dependent structural parameters and magnetic susceptibility data (5.82 μ_B at 293 K; 4.86 μ_B at 20 K) together indicate the existence of two crystallographically and magnetically distinct crystal lattice sites in the triclinic phase. One site of the triclinic phase (molecule **1**) is unique in that its structure is temperature dependent, whereas the second spin-admixed site (molecule **2**) has a structure which is essentially independent of temperature. This distinct site assignment has been further investigated by low-temperature Mössbauer (6, 77, 150 K) and EPR (11 K) spectroscopy which suggest different spin ground states for molecules **1** and **2**. As such, [Fe^{III}(TPP)(OSO_2CF_3)] represents the first report of spin-state isomerism in the solid state for a pentacoordinate [Fe^{III}(porphinato)X] species possessing two crystallographically, magnetically, and spectroscopically distinct sites in the same unit cell. This triclinic phase is also the first report of molecule pairs of the same porphyrin complex interacting in very different ways in the same crystal lattice, in that molecule **1** pairs form π–π dimers whereas molecule **2** pairs do not. Crystal data for [Fe^{III}(TPP)(OSO_2CF_3)] in the monoclinic phase at 293 K: space group $P2_1/a$ (No. 14), $Z = 4$, $a = 14.249(4)$ Å, $b = 17.630(4)$ Å, $c = 15.175(5)$ Å, $\beta = 97.35(3)°$. Crystal data for [Fe^{III}(TPP)(OSO_2CF_3)] in the triclinic phase: space group $P\bar{1}$ (No. 2), $Z = 4$; $a = 13.709(3)$ Å, $b = 26.230(3)$ Å, $c = 11.782(2)$ Å, $\alpha = 97.81(1)°$, $\beta = 114.84(2)°$, and $\gamma = 89.04(2)°$ at 293 K; $a = 13.474(8)$ Å, $b = 25.939(9)$ Å, $c = 11.666(9)$ Å, $\alpha = 97.91(5)°$, $\beta = 114.28(5)°$, and $\gamma = 88.98(4)°$ at 188 K.

All of the possible spin states for pentacoordinate iron(III) porphyrin complexes [Fe^{III}(por)X], where por is any porphyrinate dianion such as $(TPP)^{2-}$ and X^- is an anionic monodentate ligand, have been well characterized.[1] The high-spin state ($S = {}^5/_2$) is present when X^- is a strong to moderate field axial ligand such as a halide anion, $(SO_4H)^-$, or $(SO_3CH_3)^-$.[2-6] On the other hand, the low-spin state ($S = {}^1/_2$) has been only rarely encountered as in [Fe^{III}(TPP)(C_6H_5)], [Fe^{III}(TAP)(SH)], and [Fe^{III}(OEP)(NO)]$^+$.[7-9] Finally, the admixed-intermediate spin state ($S = {}^5/_2, {}^3/_2$) has been characterized for a few iron(III) porphyrin compounds. These complexes, in which the iron(III) ground state features quantum mechanical admixtures of a high-spin state ($S = {}^5/_2$) and of an intermediate-spin state ($S = {}^3/_2$) coupled via a spin–orbit interaction,[10-13] have moderate- to weak-field axial ligands, with the most representative example being [Fe^{III}(TPP)($OClO_3$)]. Admixed-intermediate spin compounds exhibit varying degrees of $S = {}^3/_2$ character depending on the nature of the axial ligand.[14-20]

The fact that these three spin states can be nearly equienergetic in certain iron(III) porphyrin complexes has been realized for sometime. For example, Hückel molecular orbital calculations[21] have shown that for certain iron(III) porphyrins the energies of the low-, intermediate-, and high-spin states can be nearly degenerate depending on the ligand and geometrical environment around the iron center. This result can, in turn, cause the spin state to vary in response to subtly changing conditions, although, in practice, this phenomenon has been largely observed in the crystalline state for only iron(III) porphyrin compounds of coordination number 6. For example, one such variable-spin complex, [Fe^{III}(OEP)(3-Clpy)$_2$]ClO_4 is reported to be in mostly a low-spin state at 98 K, while, at 295 K, the compound exhibits a thermal spin-equilibrium mixture of the high- (55%) and low-spin (45%) states for a crystal with a triclinic space group.[22] However, for a monoclinic phase, the compound possesses a quantum-admixed spin state ($S = {}^5/_2, {}^3/_2$).[23] A second example, which is perhaps more relevant to the present study, is that of the

* Abstract published in *Advance ACS Abstracts*, December 15, 1993.

(1) Abbreviations used: $(TPP)^{2-}$ is the dianion of *meso*-tetraphenylporphyrin; $(OEP)^{2-}$ is the dianion of octaethylporphyrin; $(TAP)^{2-}$ is the dianion of 5,10,15,20-tetrakis(*p*-methoxyphenyl)porphyrin; $(TMP)^{2-}$ is the dianion of 5,10,15,20-tetramethylporphyrin; 2-MeHIm is 2-methylimidazole; 3-Clpy is 3-chloropyridine.

(2) Hoard, J. L.; Cohen, G. H.; Glick, M. D. *J. Am. Chem. Soc.* **1967**, *89*, 1992.
(3) Anzai, K.; Hatano, K.; Lee, Y. J.; Scheidt, W. R. *Inorg. Chem.* **1981**, *20*, 2337.
(4) Hatano, K.; Scheidt, W. R. *Inorg. Chem.* **1979**, *18*, 877.
(5) Scheidt, W. R.; Lee, Y. J.; Finnegan, M. G. *Inorg. Chem.* **1988**, *27*, 4725.
(6) Li, N.; Levendis, D.; Coppens, P.; Kastner, M. E.; Carruth, L. E.; Scheidt, W. R. *Acta Crystallogr.* **1987**, *C43*, 1835.
(7) Doppelt, P. *Inorg. Chem.* **1984**, *23*, 4009.
(8) English, D. R.; Hendrickson, D. N.; Suslick, K. S.; Eigenbrodt, C. W.; Scheidt, W. R. *J. Am. Chem. Soc.* **1984**, *106*, 7258.
(9) Scheidt, W. R.; Lee, Y. J.; Hatano, K. *J. Am. Chem. Soc.* **1984**, *106*, 3191.
(10) Maltempo, M. M. *J. Chem. Phys.* **1974**, *61*, 2540.
(11) Maltempo, M. M.; Moss, T. H.; Cusanovich, M. A. *Biochim. Biophys. Acta* **1974**, *342*, 290.
(12) Maltempo, M. M. *Biochim. Biophys. Acta* **1975**, *379*, 97.
(13) Maltempo, M. M.; Moss, T. H. *Q. Rev. Biophys.* **1976**, *9*, 181.
(14) Reed, C. A.; Mashiko, T.; Bentley, S. P.; Kastner, M. E.; Scheidt, W. R.; Spartalian, K.; Lang, G. *J. Am. Chem. Soc.* **1979**, *101*, 2948.
(15) Scheidt, W. R.; Geiger, D. K.; Lee, Y. J.; Reed, C. A. Lang, G. *Inorg. Chem.* **1987**, *26*, 1039.
(16) Shelly, K.; Reed, C. A.; Lee, Y. J.; Scheidt, W. R. *J. Am. Chem. Soc.* **1986**, *108*, 3117.
(17) Shelly, K.; Bartczak, T.; Scheidt, W. R.; Reed, C. A. *Inorg. Chem.* **1985**, *24*, 4325.
(18) Gupta, G. P.; Lang, G.; Lee, Y. J.; Scheidt, W. R.; Shelly, K.; Reed, C. A. *Inorg. Chem.* **1987**, *26*, 3022.
(19) Masuda, H.; Taga, T.; Osaki, K.; Sugimoto, H.; Yoshida, Z.; Ogoshi, H. *Inorg. Chem.* **1980**, *19*, 950.
(20) Kastner, M. E.; Scheidt, W. R.; Mashiko, T.; Reed, C. A. *J. Am. Chem. Soc.* **1978**, *100*, 666.
(21) Scheidt, W. R.; Gouterman, M. In *Physical Bioinorganic Chemistry-Iron Porphyrins*; Lever, A. B. P., Gray, H. B., Eds.; Addison-Wesley Publishing Co.: Reading, MA, 1983; Part I, pp 89–139.
(22) Scheidt, W. R.; Geiger, D. K.; Haller, K. J. *J. Am. Chem. Soc.* **1982**, *104*, 495.
(23) Scheidt, W. R.; Geiger, D. K.; Hayes, R. G.; Lang, G. *J. Am. Chem. Soc.* **1983**, *105*, 2625.

0020-1669/94/1333-1543$04.50/0

hexacoordinate [Fe^{III}(TPP)(NCS)(Py)] compound. Originally, this compound was found to crystallize as a pure low-spin complex.[24] Later studies,[25] however, revealed that the compound also crystallizes in another form with a more complex behavior characterized by two magnetically distinct sites with one site being a spin-equilibrium site between 96 and 293 K and a second site remaining high spin over the entire temperature range.

This work consists of a structural and spectroscopic study of pentacoordinate [Fe^{III}(TPP)(OSO_2CF_3)] in a monoclinic phase at 293 K and in a triclinic phase at 293 K and 188 K by single-crystal X-ray diffraction and by magnetic susceptibility and Mössbauer and EPR spectroscopies. The molecular geometry of the compound as it crystallizes in a monoclinic lattice is that of a typical five-coordinate spin-admixed iron(III) porphyrin complex with mostly $S = {}^5/_2$ character in its ground state. However, the compound presents a more complex behavior in the triclinic lattice in that the variable-temperature structural and spectroscopic investigations can be successfully correlated with a two-site model with each site having a different spin ground state. In particular, the results indicate that one of the two sites in triclinic [Fe^{III}(TPP)(OSO_2CF_3)] (molecule **1**) is a quantum mechanically spin-admixed site ($S = {}^5/_2, {}^3/_2$) with a temperature-dependent structure, while the second site (molecule **2**) is also probably a spin-admixed site but with a temperature-independent structure to suggest a mostly $S = {}^5/_2$ state at both temperatures. Previous studies of [Fe^{III}(TPP)(OSO_2CF_3)] are few,[14,26] but in general, they too have implied a spin-admixed ground state in both the solid and solution states. The present study, however, represents the first structural verification of this spin-state assignment for [Fe^{III}(TPP)(OSO_2CF_3)], with the compound also featuring an unusual spin-state isomerism in the triclinic phase.

Experimental Section

Methods and Materials. All solvents used were reagent grade. Tetrahydrofuran (THF) was dried by distillation from sodium/benzophenone. Methylene chloride was predried with anhydrous $CaCl_2$ and distilled from P_2O_5. Toluene and heptane were distilled from sodium metal. After degassing with an argon sparge, all solvents were stored under a N_2 atmosphere in a Vacuum Atmospheres drybox. [$Ag^I(OSO_2CF_3)$] (Aldrich) was used as received.

Syntheses and Crystal Growth. $TPPH_2$[27] and [Fe^{III}(TPP)Cl][28] were prepared according to literature methods. [Fe^{III}(TPP)(OSO_2CF_3)] was prepared under an argon atmosphere using Schlenk-line techniques as a precaution against moisture and subsequent formation of the (μ-oxo)-diiron compound. A mixture of [Fe^{III}(TPP)Cl] (1.0 g, 1.42 mmol), [$Ag^I(OSO_2CF_3)$] (0.36 g, 1.42 mmol), and THF (100 mL) was gently refluxed for 30 min. The mixture was then filtered to remove the AgCl which formed during the reaction. Dry heptane (200 mL) was added to the filtrate, and the filtrate was allowed to stand in a refrigerator overnight. The precipitated purple crystalline product was collected via filtration, washed with dry toluene, and dried in vacuo at room temperature overnight over P_2O_5. The product was then recrystallized from a hot toluene/heptane mixture. Yield: 28%. Anal. Calcd. for $FeC_{45}H_{28}N_4O_3SF_3$: C, 66.10; H, 3.45; N, 6.85; S, 3.92; Fe, 6.83. Found: C, 65.96; H, 3.58; N, 6.71; S, 4.01; Fe, 6.80. Elemental analyses were obtained commercially from Galbraith Laboratories, Inc., Knoxville, TN.

Single crystals of [Fe^{III}(TPP)(OSO_2CF_3)] were grown under a N_2 atmosphere in the drybox. A concentrated solution of the compound, dissolved in freshly distilled and degassed CH_2Cl_2, was first prepared. This solution was then filtered through a fine Celite frit, and 2–6 mL aliquots were placed into several 12-mL vials with snap-on plastic caps. Varying amounts of dried and degassed heptane were then layered upon each solution. The vials were set aside in the drybox for 2–3 days, after which large crystals, in both parallelpipedic and rectangular shapes, began to form in each vial. Both X-ray crystal structure determinations (293 and 188 K) on the triclinic phase were performed on the same single crystal. Furthermore, the magnetic and spectroscopic data were all collected on crushed microcrystalline samples from the same [Fe^{III}(TPP)(OSO_2CF_3)] batch which also yielded both single crystals used for the X-ray determinations. Several single crystals were indexed and their unit cells characterized to verify that both the monoclinic and triclinic phases of the compound were present in the crushed microcrystalline samples; no evidence for other crystalline phases was encountered.

Table 1. Crystallographic Data for [Fe^{III}(TPP)(OSO_2CF_3)]

temp (K)	293	293	188
formula	$C_{45}H_{28}N_4O_3F_3FeS$	$C_{45}H_{28}N_4O_3F_3FeS$	$C_{45}H_{28}N_4O_3F_3FeS$
fw	817.65	817.65	817.65
space group	$P2_1/a$ (No. 14)	$P\bar{1}$ (No. 2)	$P\bar{1}$ (No. 2)
a (Å)	14.249(4)	13.709(3)	13.474(8)
b (Å)	17.630(4)	26.230(3)	25.939(9)
c (Å)	15.175(5)	11.782(2)	11.666(9)
α (deg)	90.00	97.81(1)	97.91(5)
β (deg)	97.35(3)	114.84(2)	114.28(5)
γ (deg)	90.00	89.04(2)	88.98(4)
V (Å^3)	3781(2)	3805(1)	3678(4)
Z	4	4	4
D_{calc} (g/cm^3)	1.44	1.44	1.47
radiation (λ, Å)	Mo Kα, graphite mono. (0.710 73)	Mo Kα, graphite mono. (0.710 73)	Mo Kα, graphite mono. (0.710 73)
μ (Mo Kα) (cm^{-1})	5.105	5.075	5.246
$R(F_o$ or $F_o^2)^a$	0.062	0.055	0.066
$R_w(F_o$ or $F_o^2)^a$	0.065	0.072	0.070

^{a} $R(F_o \text{ or } F_o^2) = \sum||F_o| - |F_c||/\sum|F_o|$ and $R_w(F_o \text{ or } F_o^2) = [\sum w(|F_o| - |F_c|)^2/\sum w(F_o)^2/\sum w(F_o)^2]^{1/2}$.

Magnetic and Spectroscopic Measurements. Magnetic susceptibilities in the 20–293 K temperature range were obtained by the Faraday method, using a system described previously,[29] except for having been modified with a Scientific Instruments Model 3800 temperature indicator/controller equipped with an LFE model 4427 voltmeter monitoring a calibrated Scientific Instruments Model Si-400 silicon diode sensor. The diamagnetic correction (χ_{dia}) was calculated using Pascal's constants[30] to be -2.81×10^{-4} cgsu mol^{-1}.

^{57}Fe Mössbauer spectra were obtained (in zero magnetic field) on a crushed polycrystalline sample at 6, 77, and 150 K using a Ranger Scientific Model MS-900 Mössbauer spectrometer interfaced to an exchange gas cryostat. The cryogenic apparatus consisted of a Cryo Industries Model 8CC variable-temperature Mössbauer cryostat with a TRI Research Model T-2000 Cryo Controller. The spectrometer used an NEC APC-3 computer for data storage and curve fitting using the Ranger Scientific Mössbauer curve-fitting program. A sodium nitroprusside (SNP) spectrum collected at room temperature was used as the reference standard.

X-band electron paramagnetic resonance (EPR) spectra were recorded at 11 K on a Varian E-Line EPR spectrometer.

Crystal Structure Determination of [Fe^{III}(TPP)(OSO_2CF_3)] in the Monoclinic Phase. Preliminary X-ray Examination and Data Collection. The crystal selected for the X-ray diffraction study was a thick, purple, rectangular crystal of approximate dimensions 0.50 × 0.25 × 0.25 mm. It was mounted with epoxy on the tip of a glass fiber. Crystal data were collected (2θ–ω scans) by using a Rigaku AFC5S automated four-circle diffractometer [Rigaku CONTROL (4:1:0) Automatic Data Collection Series (Molecular Structure Corp., 1988)]. Crystallographic data are given in Table 1. Final unit cell parameters are based upon a least-squares analysis of the angular setting of 25 carefully centered reflections ($7.09° \le 2\theta \le 12.16°$). These indicated a primitive monoclinic unit cell. Laue symmetry was checked and confirmed the monoclinic Laue group $2/m$. Three standard reflections, selected to give a good distribution in χ, were measured after every 150 reflections and showed no loss in intensity by completion of data collection. Excluding standards, 9329 reflections were collected, 8982 of which were unique ($R_{int} = 0.052$); equivalent reflections were merged. Data were collected for the octant $+h,+k,\pm l$,

(24) Scheidt, W. R.; Lee, Y. J.; Geiger, D. K.; Taylor, K.; Hatano, K. *J. Am. Chem. Soc.* **1982**, *104*, 3367.
(25) Geiger, D. K.; Chunplang, V.; Scheidt, W. R. *Inorg. Chem.* **1985**, *24*, 4736.
(26) Boersma, A. D.; Goff, H. M. *Inorg. Chem.* **1982**, *21*, 581.
(27) Adler, A. D.; Longo, F. D.; Finarelli, J. D.; Goldmacher, J.; Assour, J.; Korsakoff, L. *J. Org. Chem.* **1967**, *32*, 476. Kim, J. B.; Adler, A. D.; Longo, F. R. *The Porphyrins*; Dolphin, D., Ed.; Academic Press: New York, 1978; Vol. 1, pp 85–100.
(28) Fleischer, E. B.; Palmer, J. M.; Srivastava, T. S.; Chaterjee, A. *J. Am. Chem. Soc.* **1971**, *93*, 3162.
(29) Tweedle, M. F.; Wilson, L. *J. Rev. Sci. Instrum.* **1978**, *49*, 1001.
(30) Figgis, B. N.; Lewis, J. In *Techniques of Inorganic Chemistry*; Jonassen, H. B., Weissberger, A., Eds.; Interscience Publishers: New York, 1965; p 143.

Table 2. Selected Positional Parameters for $[Fe^{III}(TPP)(OSO_2CF_3)]$ in the Monoclinic Phase

atom	x	y	z	B_{eq},[a] Å^2
Fe1	0.71532(9)	0.10321(7)	0.20814(7)	4.85(6)
N1	0.8405(4)	0.1167(3)	0.1597(3)	4.4(3)
N2	0.7811(4)	0.1328(3)	0.3284(4)	4.6(3)
N3	0.5914(4)	0.1299(3)	0.2532(4)	5.0(4)
N4	0.6476(4)	0.1193(3)	0.0819(4)	5.3(4)
O1	0.7176(4)	–0.0069(3)	0.2177(3)	6.8(3)
O2	0.6665(5)	–0.0380(4)	0.3580(4)	9.4(4)
S1A	0.6775(3)	–0.0622(3)	0.2668(3)	7.6(3)
S1B	0.7397(7)	–0.0574(5)	0.3019(6)	8.6(6)
O3A	0.6104(9)	–0.113(1)	0.2159(7)	12.1(7)
O3B	0.841(2)	–0.116(1)	0.334(2)	6.3(9)

[a] $B_{eq} = (8\pi^2/3)\sum_{i=1}^{3}\sum_{j=1}^{3}U_{ij}a_i^*a_j^*\vec{a}_i\vec{a}_j$.

ranging as h, 0 to 19, k, 0 to 23, and 1, –20 to 20, with $2\theta_{max} = 55.0°$. All independent data to $[(\sin\theta)/\lambda]_{max} = 0.65$ were measured.

Structure Solutions and Refinements. Laue symmetry and systematic absences indicated the space group $P2_1/a$ (No. 14). The structure was solved by direct methods using the program MITHRIL[31] which located the Fe atom. The rest of the non-hydrogen atoms were located using the program DIRDIF.[32] Refinement was performed using the TEXSAN (v. 2.0) structure analysis package (Molecular Structure Corp., 1988). Hydrogen atoms were included in the structure factor calculation in idealized positions (C–H = 0.95 Å) and were assigned isotropic thermal parameters which were 20% greater than the B equivalent value of the atom to which they were bonded. All non-hydrogen atoms were assigned anisotropic thermal parameters except for the CF_3 group, which was treated as a rigid body in the least-squares refinement. The trifluoromethanesulfonate ligand was found to be disordered, except for the bridging oxygen (O1) atom. Fractional atoms for the CF_3SO_2 group were allowed to occupy two possible atom positions (based on a Fourier difference map). The occupancy factor of the CF_3SO_2 group in one orientation was refined to 0.66. The complement of each of these atoms was constrained to an occupancy factor of 0.34. The data were corrected for absorption (ψ scans[33]) and for Lorentz/polarization effects but not for decay. The final cycle of full-matrix least-squares refinement converged with unweighted and weighted agreement factors of $R = \sum\|F_o| - |F_c\|/\sum|F_o| = 0.062$ and $R_w = [\sum w(|F_o| - |F_c|)^2/\sum w(F_o)^2]^{1/2} = 0.065$. The ratio of maximum least-squares shift to error in the final refinement cycle, $(\Delta/\sigma)_{max}$, was 0.05. The maximum positive ($(\Delta\rho)_{max}$) and maximum negative ($(\Delta\rho)_{min}$) electron density peaks on the final difference Fourier map corresponded to 0.40 and –0.41 e/Å^3, respectively. Selected final values of atomic coordinates are given in Table 2. The analytical form of the scattering factors for the appropriate neutral atoms were corrected for both the real ($\Delta f'$) and imaginary ($i\Delta f''$) components of anomalous dispersions.[34]

Data collection and refinement parameters, atomic coordinates, listings of bond lengths and angles, final values of the ansiotropic thermal parameters, fixed hydrogen atom coordinates, and derived coordinates of the CF_3 rigid groups can be found as supplementary material.

Crystal Structure Determination of $[Fe^{III}(TPP)(OSO_2CF_3)]$ in the Triclinic Phase. Preliminary X-ray Examination and Data Collection. A rather large (0.3 × 0.4 × 0.8 mm), purple, cut parallelpipedic single crystal of $[Fe^{III}(TPP)(OSO_2CF_3)]$ was mounted on the tip of a glass fiber with epoxy cement and used for both temperatures. Measurements at 188 K were made using a fixed-tube, low-temperature attachment designed and manufactured by Molecular Structure Corp.; temperature control during data collection was ±2 °C. Preliminary examination of the crystal revealed a four-molecule triclinic unit cell. A Delaunay reduction did not show any hidden symmetry. The unit cell parameters were derived from the least-squares best fit of 50 carefully centered reflections ($0.00° \le 2\theta \le 11.73°$ at 293 K; $6.66° \le 2\theta \le 13.17°$ at 188 K). These indicated a primitive triclinic unit cell. Intensity data were collected (ω scans) at both temperatures using a Rigaku AFC5S automated four-circle diffractometer [CONTROL (4:1:0) Automatic Data Collection Series (Molecular Structure Corp., 1988)]. Crystal data are given in Table 1 for the data collected at 293 and 188 K. The intensities of three representative standard reflections were measured every 150 reflections to monitor and control crystal alignment and decomposition. These standard reflections showed no significant variation throughout data collection at 293 and 188 K. At 293 K, 18 171 reflections were collected excluding standards, 17 440 of which were unique ($R_{int} = 0.020$). At 188 K, 17 610 reflections were collected excluding standards, 16 893 of which were unique ($R_{int} = 0.074$). Equivalent reflections were merged in both cases. For both temperatures, data were collected for the octants $+h,\pm k,\pm l$, ranging as h, 0 to 18, k, –34 to 34, and l, –15 to 15, with $2\theta_{max} = 55.1°$. All independent data to $[(\sin\theta)/\lambda]_{max} = 0.65$ were measured.

Table 3. Selected Positional Parameters for $[Fe^{III}(TPP)(OSO_2CF_3)]$ at 293 K in the Triclinic Phase

atom	x	y	z	B_{eq},[a] Å^2
Fe1	0.03849(5)	0.39520(2)	0.93393(6)	3.05(2)
S1	0.1683(1)	0.34476(5)	0.7746(1)	4.56(5)
O1	0.0860(2)	0.3474(1)	0.8214(3)	4.3(1)
O2	0.2369(3)	0.3897(1)	0.8149(4)	6.8(2)
O3	0.1289(3)	0.3228(2)	0.6455(4)	8.1(2)
C1S	0.2528(5)	0.2966(3)	0.8592(7)	6.1(3)
F1	0.3010(4)	0.3121(2)	0.9800(4)	12.0(3)
F2	0.2001(4)	0.2532(2)	0.8389(6)	12.4(3)
F3	0.3302(3)	0.2857(2)	0.8224(4)	8.9(2)
N1	–0.1183(3)	0.3868(1)	0.8134(3)	3.0(1)
N2	0.0435(3)	0.4642(1)	0.8789(3)	3.1(1)
N3	0.0118(3)	0.3435(1)	1.0306(3)	3.0(1)
N4	0.1808(3)	0.4153(1)	1.0821(3)	3.2(1)
Fe2	0.80158(5)	0.09103(2)	0.42772(6)	3.32(2)
S2	0.5740(1)	0.12605(7)	0.4188(2)	6.94(8)
O4	0.6537(2)	0.0904(1)	0.4266(3)	4.9(1)
O5	0.5053(4)	0.1076(2)	0.4699(5)	10.6(3)
O6	0.6166(4)	0.1789(2)	0.4613(6)	10.6(3)
C2S	0.4885(7)	0.1240(5)	0.252(1)	10.9(6)
F4	0.4113(6)	0.1539(4)	0.2408(8)	23.3(6)
F5	0.443(1)	0.0853(3)	0.1954(6)	24.7(7)
F6	0.5344(5)	0.1430(3)	0.1917(6)	17.4(5)
N5	0.7831(3)	0.1293(1)	0.2821(3)	3.7(1)
N6	0.8735(3)	0.1570(1)	0.5465(3)	3.3(1)
N7	0.8819(3)	0.0512(1)	0.5748(3)	3.3(1)
N8	0.7863(3)	0.0243(1)	0.3092(3)	3.6(1)

[a] See footnote *a* of Table 2.

Structure Solutions and Refinements. The structure was initially solved using the data set collected at 293 K by using the direct methods program MITHRIL[31] which located the Fe atoms. All remaining non-hydrogen atoms were located using the direct methods program DIRDIF[32] and further refined by difference Fourier syntheses using the TEXSAN (v. 2.0) structure analysis package (Molecular Structure Corp., 1988). On the basis of packing considerations, a statistical analysis of intensity distribution, and the successful solution and refinement of the structure, the space group was determined to be $P\bar{1}$ (No. 2). Hydrogen atoms were included in the structure factor calculation in idealized positions (C–H = 0.95 Å) and were assigned isotropic thermal parameters which were 20% greater than the B equivalent value of the atom to which they were bonded. All non-hydrogen atoms were assigned anisotropic temperature factors and the refinement carried to convergence. An empirical ψ-scan absorption correction,[33] based on azimuthal scans of several reflections, was applied. The data were also corrected for Lorentz and polarization effects. A decay correction was not applied. The final cycle of full-matrix least-squares refinement converged with unweighted and weighted agreement factors of $R = \sum\|F_o| - |F_c\|/\sum|F_o| = 0.055$ and $R_w = [\sum w(|F_o| - |F_c|)^2/\sum w(F_o)^2]^{1/2} = 0.072$. $(\Delta/\sigma)_{max} = 0.01$, $(\Delta\rho)_{max} = 0.75$ e/Å^3, and $(\Delta\rho)_{min} = -0.72$ e/Å^3. Selected final values of atomic coordinates are given in Table 3. The analytical form of the scattering factors for the appropriate neutral atoms were corrected at all temperatures for both the real ($\Delta f'$) and imaginary ($i\Delta f''$) components of anomalous dispersions.[34]

The $[Fe^{III}(TPP)(OSO_2CF_3)]$ structure was also determined at 188 K by using the previously determined coordinates of the 293 K structure to establish phases. As for the case of the 293 K structure, an empirical ψ-scan absorption correction[33] was applied. The data were also corrected for Lorentz and polarization effects. Refinement was carried out exactly as before. At convergence, $R = 0.066$, $R_w = 0.070$, $(\Delta/\sigma)_{max} = 0.02$, $(\Delta\rho)_{max} = 0.45$ e/Å^3, and $(\Delta\rho)_{min} = -0.63$ e/Å^3. Selected atomic coordinates are reported in Table 4.

(31) Gilmore, C. J. *J. Appl. Crystallogr.* **1984**, *17*, 42.
(32) Beurskens, P. T. DIRDIF: Direct Methods for Difference Structures-an Automatic Procedure for Phase extension and refinement of difference structure factors. Technical Report 1984/1. Crystallography Laboratory, Toernooiveld, 6525 Ed Nijmegen, The Netherlands.
(33) North, A. C. T.; Phillips, D. C.; Mathews, F. S. *Acta Crystallogr.* **1968**, *A24*, 351.
(34) Cromer, D. T.; Weber, J. T. *International Tables for X-ray Crystallography*; The Kynoch Press: Birmingham, England, 1974; Vol. 4, Table 2.2A.

Table 4. Selected Positional Parameters for [Fe^{III}(TPP)(OSO_2CF_3)] at 188 K in the Triclinic Phase

atom	x	y	z	B_{eq},[a] Å^2
Fe1	0.0352(1)	0.39540(5)	0.9350(1)	2.22(6)
S1	0.1641(2)	0.3436(1)	0.7708(3)	3.2(1)
O1	0.0820(5)	0.3461(2)	0.8212(6)	2.8(3)
O2	0.2340(6)	0.3893(3)	0.8118(7)	4.3(3)
O3	0.1251(6)	0.3214(3)	0.6413(7)	5.0(4)
C1S	0.252(1)	0.2956(5)	0.857(1)	4.3(6)
F1	0.2981(7)	0.3110(3)	0.9784(7)	7.7(4)
F2	0.1960(6)	0.2512(3)	0.8353(9)	7.8(4)
F3	0.3288(5)	0.2842(3)	0.8164(7)	5.9(3)
N1	−0.1207(6)	0.3868(3)	0.8154(7)	1.9(3)
N2	0.0419(6)	0.4646(3)	0.8781(7)	1.9(3)
N3	0.0083(6)	0.3432(3)	1.0326(7)	2.1(3)
N4	0.1782(6)	0.4144(3)	1.0786(7)	2.0(3)
Fe2	0.7986(1)	0.09074(5)	0.4280(1)	2.50(6)
S2	0.5719(3)	0.1249(1)	0.4201(4)	5.5(2)
O4	0.6502(5)	0.0887(2)	0.4237(7)	3.4(3)
O5	0.5002(7)	0.1066(4)	0.471(1)	8.0(5)
O6	0.6144(7)	0.1783(3)	0.463(1)	7.6(5)
C2S	0.485(1)	0.120(1)	0.249(2)	8(1)
F4	0.406(1)	0.1541(7)	0.239(1)	19(1)
F5	0.447(2)	0.0790(6)	0.194(1)	22(1)
F6	0.5344(9)	0.1430(5)	0.192(1)	12.5(7)
N5	0.7781(6)	0.1294(3)	0.2798(7)	2.4(3)
N6	0.8687(6)	0.1572(3)	0.5450(7)	2.2(3)
N7	0.8806(6)	0.0511(3)	0.5764(7)	2.2(3)
N8	0.7854(6)	0.0231(3)	0.3075(8)	2.7(3)

[a] See footnote *a* of Table 2.

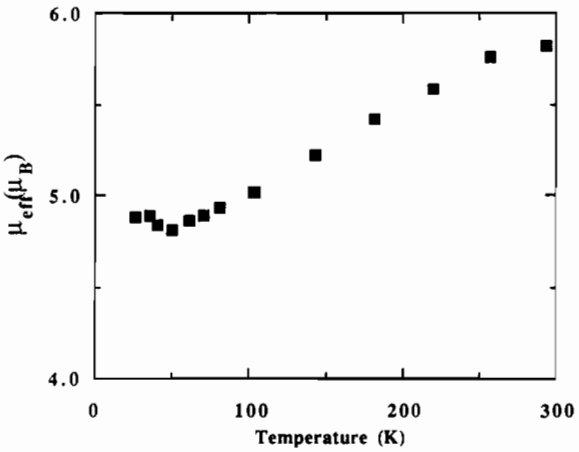

Figure 1. Plot of magnetic moment (μ_{eff}) vs temperature for [Fe^{III}(TPP)(OSO_2CF_3)].

Complete data collection and refinement parameters, atomic coordinates, listings of bond lengths and angles, final values of the anisotropic thermal parameters, and fixed hydrogen atom coordinates for the 293 and 188 K structures can be found as supplementary material.

Results and Discussion

As can be seen from Figure 1, the magnetic moment of crystalline [Fe^{III}(TPP)(OSO_2CF_3)] gradually decreases from a value of 5.82 μ_B at 293 K to a value of ca. 4.85 μ_B by 60 K and plateaus at this value down to 20 K. Such non-Curie behavior is unusual for monomeric iron(III) porphyrin compounds.[35] To help ascertain the source of this anomalous magnetic behavior, a temperature-dependent X-ray crystal structure determination of [Fe^{III}(TPP)(OSO_2CF_3)] was undertaken: at 293 K (5.82 μ_B) for both triclinic and monoclinic crystal systems and at 188 K (5.44 μ_B) for the triclinic phase. The structure at 188 K represents the point at which ~40% of the observed change in μ_{eff} has been effected.[36]

Structural Considerations. In the past several years, many porphyrin derivatives have been systematically studied and a number of spin-state/stereochemical relationships discovered for iron porphyrins have been proposed to be a "final arbiter" of the spin state.[37,38] Trends observed in bond distance variations, iron out-of-plane displacements, and porphinato core expansions/contractions have been attributed to the depopulation of the antibonding iron $d_{x^2-y^2}$ orbital in states of lower spin. Specifically, the short average distance from the Fe atom to the porphinato core N atoms (Fe–N_p) and the displacement of the Fe atom from the center of the mean plane of the 24-atom porphyrin core (Fe···$C_{t'}$) are the structural signature of a high- or admixed intermediate-spin state for the pentacoordinate iron(III) atom.[37,38] For the high-spin case, the typical Fe–N_p and Fe···$C_{t'}$ distances are ≥2.045 and ≥0.42 Å, respectively. Such long distances, as well as the size of the central hole of the porphinato core, indicate that the iron $d_{x^2-y^2}$ and d_{z^2} orbitals are both occupied and that the spin state is $S = {}^5/_2$.[18,19,38,39] On the other hand, values reported for five-coordinate admixed-spin iron(III) porphyrinates are in the range 1.961–2.038 Å for Fe–N_p and 0.10–0.36 Å for the displacements of the iron atom, varying according to the amount of $S = {}^3/_2$, ${}^5/_2$ character present in the system. These shorter distances are indicative of a partially occupied, $d_{x^2-y^2}$ antibonding orbital due to it being raised in energy relative to the d_{z^2}, d_{xy}, d_{yz}, and d_{xz} orbitals because of the proximity (and subsequent repulsion) between the $d_{x^2-y^2}$ electron and the sp^2 lone pair of electrons of the equatorial porphyrin nitrogens.[14,18,19]

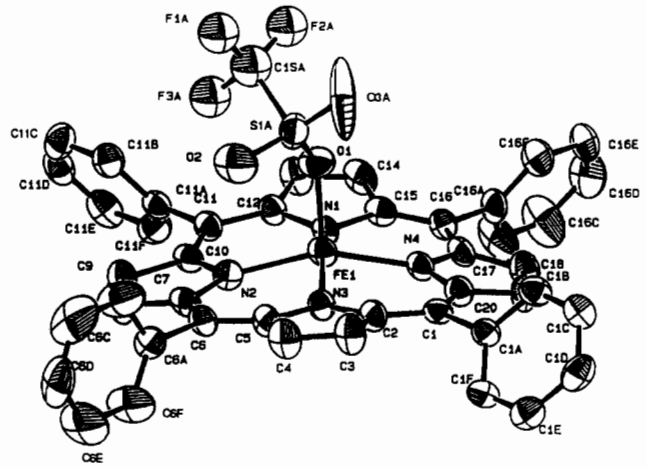

Figure 2. ORTEP drawing of [Fe^{III}(TPP)(OSO_2CF_3)] at 293 K in the monoclinic phase. Ellipsoids are contoured at the 50% probability level.

[Fe^{III}(TPP)(OSO_2CF_3)] at 293 K in the Monoclinic Phase. The molecular structure for [Fe^{III}(TPP)(OSO_2CF_3)] at 293 K in the monoclinic phase is presented in Figure 2 as an ORTEP drawing which also presents the numbering scheme used for the atoms. Selected bond distances and angles are presented in Tables 5 and 6, respectively. The average value of the displacement of the iron atom, 0.38 Å, and the average Fe–N_p distance of 2.030(6) Å are both at the upper end of the range observed for iron(III) porphyrinates in the admixed-spin state (see Table 7 for a comparison of the coordination group parameters for this

(35) Gregson, A. K. *Inorg. Chem.* **1981**, *20*, 81.

(36) A crystal structure determination on the same single crystal was also attempted at 103 K which corresponds to 5.02 μ_B in the magnetic moment curve where >80% of the observed change in μ_{eff} has been effected. The data set at this temperature is not as acceptable as the other two, probably due to ice buildup on the crystal during data collection. Crystal data for [Fe^{III}(TPP)(OSO_2CF_3)] in the triclinic phase at 103 K: space group $P\bar{1}$ (No. 2), $Z = 4$; $a = 13.490(9)$ Å, $b = 25.957(9)$ Å, $c = 11.636(9)$ Å, $\alpha = 98.34(5)°$, $\beta = 114.02(6)°$, and $\gamma = 88.95(5)°$. Non-hydrogen atoms were assigned anisotropic thermal parameters except for the CF_3 group and all the phenyl groups which were treated as rigid bodies in the refinement. This model has $R = 0.098$ and $R_w = 0.118$.

(37) Scheidt, W. R.; Lee, Y. J. In *Structure and Bonding 64-Metal Complexes with Tetrapyrrole Ligands I*; Buchler, J. W., Ed.; Springer-Verlag: New York, 1987; pp 1–70.

(38) Scheidt, W. R.; Reed, C. A. *Chem. Rev.* **1981**, *81*, 543.

(39) Kellet, P. J.; Pawlik, M. J.; Taylor, L. F.; Thompson, R. G.; Levstik, M. A.; Anderson, O. P.; Strauss, S. H. *Inorg. Chem.* **1989**, *28*, 440.

Table 5. Selected Intramolecular Distances (Å) for [Fe^{III}(TPP)(OSO$_2$CF$_3$)] at 293 K in the Monoclinic Phase

Fe1–N1	2.029(6)	O2–S1A	1.475(8)
Fe1–N2	2.011(6)	O2–S1B	1.47(1)
Fe1–N3	2.029(6)	S1A–O3A	1.46(1)
Fe1–N4	2.051(6)	S1A–C1SA	1.857(9)
Fe1–O1	1.946(6)	S1B–O3B	1.59(1)
O1–S1A	1.393(7)	S1B–C1SB	1.76(1)
O1–S1B	1.46(1)		

Table 6. Selected Intramolecular Bond Angles (deg) for [Fe^{III}(TPP)(OSO$_2$CF$_3$)] at 293 K in the Monoclinic Phase

N1–Fe1–N2	88.2(2)	O1–S1B–O2	105.1(6)
N1–Fe1–N3	159.9(2)	O1–S1B–O3B	129(1)
N1–Fe1–N4	88.6(2)	O2–S1B–O3B	126(1)
N1–Fe1–O1	97.8(2)	O1–S1B–C1SB	105.5(6)
N2–Fe1–N3	87.6(2)	O2–S1A–O3A	122.3(6)
N2–Fe1–N4	157.0(2)	O1–S1A–C1SA	93.8(4)
N2–Fe1–O1	100.9(2)	O1–S1A–O3A	115.6(6)
N3–Fe1–N4	87.6(2)	O1–S1A–O2	113.6(4)
N3–Fe1–O1	102.3(3)	Fe1–O1–S1B	129.1(5)
N4–Fe1–O1	102.1(2)	Fe1–O1–S1A	137.1(4)
O3A–S1A–C1SA	106.8(7)		

complex with those of other structurally characterized related compounds). These distances are in accord with an iron(III) center in an admixed intermediate-spin state of predominant $S = {}^5/_2$ character.[13,18,40] Molecules of [Fe^{III}(TPP)(OSO$_2$CF$_3$)] in the monoclinic lattice interact in pairs in the solid state. To investigate the possibility of these pairs forming porphyrin π–π dimers and that the two iron(III) ions of the pairs are coupled through the π systems which might result in EPR silence,[15,18,40] the core to core interactions have been analyzed in detail. Figure 3 defines the relevant distances and angles to be considered when evaluating π–π systems. The two main guidelines for π–π complex formation between porphyrin rings in the solid state are an MPS of less than 4.0 Å and at least some overlap of the two porphyrin cores.[37,41] These interactions for [Fe^{III}(TPP)(OSO$_2$CF$_3$)] in the monoclinic lattice are shown in Figure 4 and 5. For this molecule, the core planes are slightly tilted, with a dihedral angle of 8.7°, and the relevant parameters are as follows: $C_{t'}\cdots C_{t'} = 7.50$ Å, LS = 5.86 Å and SA = 51.4°. These values, along with Figure 5, clearly show that there is very little overlap of the porphyrin macrocycles in adjacent molecules. Also, a mean plane separation of 4.67 Å and an Fe···Fe distance of 8.806(2) Å are both long for any significant π–π porphyrin interaction. This analysis leads to the conclusion that the iron(III) centers in this crystalline phase are essentially noninteracting and should, therefore, present an EPR signature characteristic of the iron(III) ground state (see below).[15,18,40,42]

[Fe^{III}(TPP)(OSO$_2$CF$_3$)] at 293 K in the Triclinic Phase. The fact that the metal centers of the [Fe^{III}(TPP)(OSO$_2$CF$_3$)] molecules of the triclinic unit cell were in two crystallographically distinct lattice sites became apparent as the structure was first solved using the data collected at 293 K. Hereafter, these two distinct molecular sites are designated as molecule **1** and molecule **2**. ORTEP drawings of these two molecules are displayed in Figures 6 and 7, which also present the numbering scheme used for the atoms of the coordination group. Tables 8 and 9 list selected individual bond distances and angles, respectively.

Molecule **2** at 293 K has an average Fe–N$_p$ distance of 2.038(6) Å and a significant out-of-plane displacement of 0.430(4) Å. These values fall in the lower end of the range of those found for high-spin iron(III) porphyrin compounds reported in the literature,[37,38] as summarized in Table 7. These distances indicate that the spin state of the iron(III) center in molecule **2** is essentially $S = {}^5/_2$.[18,19,38,39] This, however, is not the case for molecule **1**, which has an average Fe–N$_p$ distance of 2.014(3) Å and a Fe···C$_{t'}$ distance of 0.321(3) Å at 293 K. This structural information leads to the conclusion that molecule **1** probably possesses an iron(III) center in a quantum mechanically spin-admixed ($S = {}^5/_2, {}^3/_2$) state with a fairly large component of $S = {}^5/_2$ character at 293 K, as suggested by the comparative structural parameters shown in Table 7.

Figures 8 and 9 show formal diagrams of the porphinato skeleton in molecules **1** and **2** at 293 and 188 K. At both temperatures, molecule **1** and molecule **2** present nearly idealized D_{2d}-ruffled cores. Molecule **1** displays a saddle-shaped ("Sad") core[37] with large deviations from planarity in the individual atoms. This substantial ruffling of the 24-atom skeleton accompanies the relatively short Fe–N$_p$ and Fe···C$_{t'}$ distances which are characteristic of spin-admixed systems with a significant amount of $S = {}^3/_2$ character.[18] Additionally, this Sad ruffling pattern is often indicative of dimer pairing of adjacent porphyrin molecules since it sterically allows for stronger interporphyrin interactions.[18,37] The dihedral angles between the phenyl groups and the mean plane of the 24-atom porphyrin core are 61.2, 86.5, 83.1, and 48.2°. On the other hand, molecule **2** displays a ruffled ("Ruf") conformation with near-S_4 symmetry.[14,37] Deviations from planarity are much less evident for this molecule, and this allows for longer Fe–N$_p$ and Fe···C$_{t'}$ distances consonant with more $S = {}^5/_2$ spin character. The dihedral angles between the peripheral phenyl groups and the mean plane of the core are 66.7, 72.0, 83.2, and 75.7°; these are well within the range of values usually observed for either weakly or noninteracting porphyrin molecules. This Ruf conformation for molecule **2** is also consistent with a weaker intermolecular association between porphyrin molecules than for molecule **1**.[37]

Detailed consideration of possible π–π dimer interaction between both molecules in this structure have yielded some interesting results, especially when compared to those in previously reported π–π porphyrin dimers,[37] in general, and to [Fe^{III}(TPP)(OSO$_2$CF$_3$)] in the monoclinic phase with very little dimer interactions, in particular. Figure 10 shows a computer-generated edge-on view of the π–π dimer formed by molecule **1** in which the planes of the porphyrin cores are nearly perpendicular to the plane of the page. Figure 11 presents a projection of the two interacting porphyrin cores, and the strong overlap between them is evident. For molecule **1**, the two core planes are exactly parallel to each other with an Fe···Fe distance of 5.71 Å, MPS = 3.82 Å, a $C_{t'}\cdots C_{t'}$ distance of 4.86 Å, LS = 3.01 Å, and SA = 38.23°. All these values are well within the range observed in previously reported closely interacting π–π dimers of porphyrin molecules.[37] The MPS and LS distances classify molecule **1** as a type I π–π dimer which features an intermediate-strength interaction between the cores.[37] It was previously believed that the bulky phenyl groups would inhibit π–π dimer formation between tetraphenylporphyrin derivatives.[43] However, the reported structure[18] for [Fe^{III}(TPP)(HB$_{11}$CH$_{11}$)], along with the present example for molecule **1**, is clear evidence that closely interacting π–π dimers can form between iron^{III}(TPP)-type molecules provided that the two dihedral angles between the phenyl groups and the core, specifically the ones which lie in the N–Fe–N plane of the other interacting complex, are in the 40–60° range. It is also important to note that the dimers in molecule **1** and those in the (B$_{11}$CH$_{12}$)$^-$ complex interact in an almost identical spatial arrangement. For the latter compound,[18] MPS = 3.83 Å, the Fe···Fe distance is 5.49 Å, and the interacting dimer molecules are positioned with respect to each other in exactly the same fashion as that shown in Figures 10 and 11 for molecule **1**. Most importantly, in [Fe^{III}(TPP)(HB$_{11}$CH$_{11}$)] the iron(III) spins are magnetically coupled ($J = -3.0$ cm^{-1}) resulting, as it is the case with other

(40) Gupta, G. P.; Lang, G.; Schedit, W. R.; Geiger, D. K.; Reed, C. A. *J. Chem. Phys.* **1986**, *85*, 5212.
(41) Hunter, C. A.; Sanders, K. M. *J. Am. Chem. Soc.* **1990**, *112*, 5525.
(42) Gupta, G. P.; Lang, G.; Scheidt, W. R.; Shelly, K.; Reed, C. A. *J. Chem. Phys.* **1987**, *86*, 5288.
(43) Scheidt, W. R.; Geiger, D. K.; Lee, Y. J.; Reed, C. A.; Lang, G. *J. Am. Chem. Soc.* **1985**, *107*, 5693.

Table 7. Coordination Group Parameters (Distances in Å; Standard Deviations in Parentheses) and Symmetry for $[Fe^{III}(TPP)(OSO_2CF_3)]$ at 293 and 188 K in the Monoclinic and Triclinic Phases and Comparisons with Representative Values Reported for Other Five Coordinate Admixed-Spin and High-Spin Iron(III) Porphyrinates

complex	% $S = {}^3/_2$[a]	Fe–N_p[b]	Fe···C_t[c]	C_t···N[d]	Fe–X[e]	lattice	space group	ref
$[Fe(TPP)(OCOCF_3)]$	0	2.054(5)	0.48	2.00	1.921(4)	monoclinic	$P2_1/a$	54, 55
$[Fe(TPP)(OSO_3H)]$	0	2.042(10)	0.42	2.00	1.926(11)	monoclinic	$P2/c$	5
$[Fe(OEP)(2\text{-}MeHIm)]ClO_4$	2	2.038(6)	0.36	2.01	2.068(4)	monoclinic	$P2_1/n$	18, 43
$[Fe(TPP)(OSO_2CF_3)]$								
molecule **2** (293 K)	*f*	2.038(6)	0.43	1.99	2.022(3)	triclinic	$P\bar{1}$	this work
molecule **2** (188 K)	*f*	2.037(7)	0.44	1.99	1.982(7)	triclinic	$P\bar{1}$	this work
$[Fe(TPP)(OSO_2CF_3)]$	*f*	2.030(6)	0.38	1.99	1.946(6)	monoclinic	$P2_1/a$	this work
$[Fe(TPP)(OSO_2CF_3)]$								
molecule **1** (293 K)	*g*	2.014(2)	0.32	1.99	2.000(3)	triclinic	$P\bar{1}$	this work
molecule **1** (188 K)	*g*	1.994(21)	0.29	1.97	1.996(6)	triclinic	$P\bar{1}$	this work
$[Fe(TPP)(OClO_3)]$	65	2.001(5)	0.30	1.98	2.029(4)	monoclinic	$P2_1/n$	14
$[Fe(OEP)(3\text{-}Clpy)]ClO_4$	81	1.979(6)	0.22	1.97	2.126(5)	monoclinic	$C2/c$	15
$[Fe(TPP)(HB_{11}CH_{11})]$	92	1.961(5)	0.10	1.96	1.82(4)	triclinic	$P\bar{1}$	18
$[Fe(TPP)(FSbF_5)]$	98	1.978(3)	0.15	1.97	2.105(3)	orthorombic	$Pna2_1$	17

[a] Values from spectroscopic data given in the references. [b] Fe–N_p is the distance from the Fe atom to the porphinato core N atoms. [c] Fe–C_t is the distance from the Fe atom to the center of the mean plane of the 24-atom core. [d] C_t···N is the radius of the central hole of the porphinato core. [e] Fe–X is the distance from the Fe atom to the axial ligand. [f] % $S = {}^3/_2$ character can be estimated from EPR parameters as discussed in the text. [g] Molecule **1** is EPR silent; its % $S = {}^3/_2$ character varies with temperature. See discussion in the text.

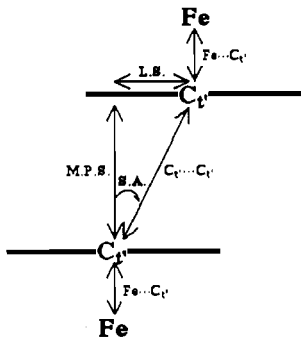

Figure 3. Diagram illustrating the definition of mean plane separation (MPS), the lateral shift (LS), the center to center distance (C_t···$C_{t'}$), and the shift angle (SA).

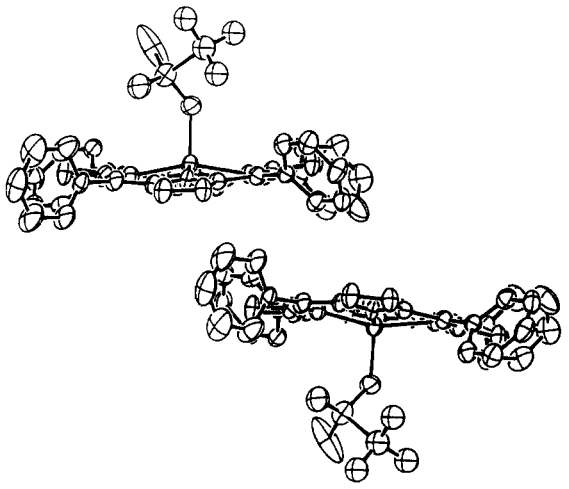

Figure 4. Edge-on view of a dimer in $[Fe^{III}(TPP)(OSO_2CF_3)]$ at 293 K in the monoclinic phase.

reported five-coordinated iron(III) porphyrin derivatives which exhibit strong π–π interacting dimers in the solid state, in the lack of an EPR signal.[15,18,40,42,43] Thus, we believe that this is probably the case for molecule **1** in $[Fe^{III}(TPP)(OSO_2CF_3)]$ in the triclinic phase.

Surprisingly, molecule **2** of the same unit cell is not involved in a significant π–π dimer interaction. The relevant distances for this molecule are as follows: Fe···Fe = 6.99 Å, C_t···$C_{t'}$ = 5.73 Å, MPS = 3.96 Å, LS = 4.14 Å, and SA = 46.28°. These values place molecule **2** in the group W dimers whose interactions are uncertain at best.[37] Computer-generated views of these dimer pairs are shown in Figures 12 and 13. These figures show how

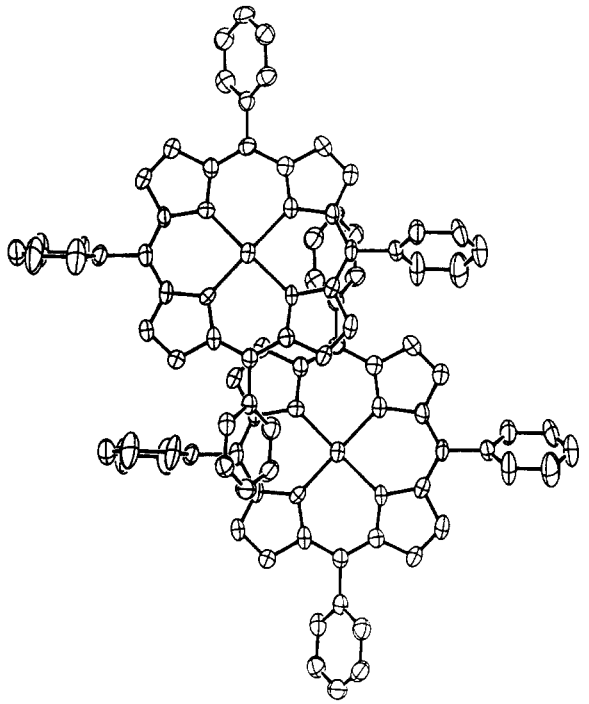

Figure 5. Projection of the two porphyrin planes within a dimer of $[Fe^{III}(TPP)(OSO_2CF_3)]$ at 293 K in the monoclinic phase.

molecule **2** packs in a very different fashion when compared to molecule **1**. Not only there is no overlap of the 24-atom cores but a phenyl group with a dihedral angle of 75.7° is positioned almost atop the central iron(III) atom, thus sterically preventing any closer contact and interaction between molecules. It should be noted that there is even less overlap in the present case (see Figure 13) than that found in a "typical" group W interaction as that exhibited by [Ti(OEP)O].[37,44] Therefore, it is reasonable that molecule **2** should be EPR active.

$[Fe^{III}(TPP)(OSO_2CF_3)]$ at 188 K in the Triclinic Phase. The results of the low-temperature crystal-structure study were especially interesting and rather surprising. Listings of selected bond distances and angles for $[Fe^{III}(TPP)(OSO_2CF_3)]$ at 188 K are given in Tables 10 and 11, respectively. ORTEP plots of molecules **1** and **2** are available as supplementary material. The coordination group geometry of molecule **1** at low temperature seems to be different from that of molecule **2**. It is also evident

(44) Guilard, R.; Latour, J. M., Lecomte, C.; Marchon, J. C.; Protas, J.; Ripoll, D. *Inorg. Chem.* **1978**, *17*, 1228.

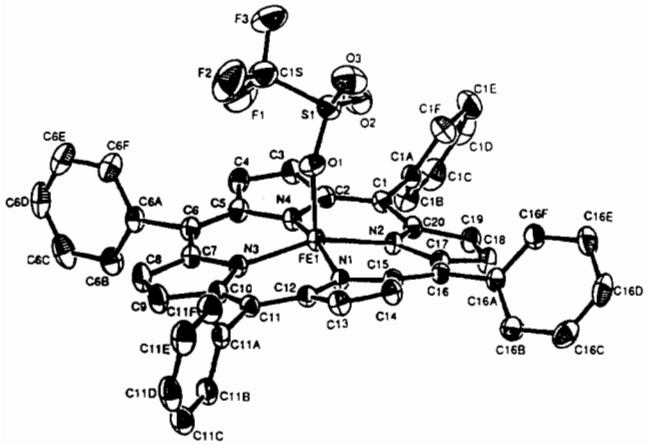

Figure 6. ORTEP drawing of molecule **1** in $[Fe^{III}(TPP)(OSO_2CF_3)]$ at 293 K in the triclinic phase. Ellipsoids are contoured at the 50% probability level.

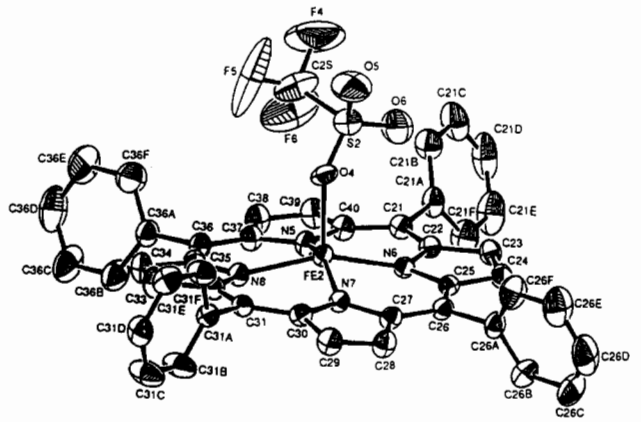

Figure 7. ORTEP drawing of molecule in **2** in $[Fe^{III}(TPP)(OSO_2CF_3)]$ at 293 K in the triclinic phase. Ellipsoids are contoured at the 50% probability level.

Table 8. Selected Intramolecular Distances (Å) for $[Fe^{III}(TPP)(OSO_2CF_3)]$ at 293 K in the Triclinic Phase

Fe1–O1	2.000(3)	Fe2–O4	2.022(3)
Fe1–N1	2.012(3)	Fe2–N5	2.029(4)
Fe1–N2	2.016(3)	Fe2–N6	2.042(4)
Fe1–N3	2.015(3)	Fe2–N7	2.038(3)
Fe1–N4	2.014(3)	Fe2–N8	2.041(4)
S1–O1	1.447(3)	S2–O4	1.408(3)
S1–O2	1.418(4)	S2–O5	1.433(5)
S1–O3	1.420(4)	S2–O6	1.451(5)
S1–C1S	1.805(6)	S2–C2S	1.81(1)
C1S–F1	1.299(7)	C2S–F4	1.28(1)
C1S–F2	1.298(7)	C2S–F5	1.16(1)
C1S–F3	1.318(6)	C2S–F6	1.28(1)

that molecule **1** undergoes structural reorganization with temperature, while molecule **2** does not.

A comparison of the Fe–N_p and Fe···$C_{t'}$ distances for molecule **2** with the reported structural parameters of other known high-spin and spin-admixed iron(III) porphinato complexes in Table 7 implies that the iron(III) center in molecule **2** is essentially $S = {}^5/_2$ at 188 K.[45] This is not the case for molecule **1** in that the decrease in temperature seems to have induced changes in the immediate coordination environment of the metal center when compared to the room-temperature structure. The Fe–N_p distance for molecule **1** at 188 K is 1.994(21) and its Fe···$C_{t'}$ distance is 0.29(1) Å.[46] An unoccupied (or partially unoccupied) $d_{x^2-y^2}$ orbital results in shorter Fe–N_p and $C_{t'}$···N distances. This is evidenced by the reported Fe–N_p distances for pure low-spin (empty $3d_{x^2-y^2}$ orbital) pentacoordinate iron(III) porphyrin compounds which average 1.99 Å, while their $C_{t'}$···N distances average 1.97 Å.[7-9] Moreover, for the series of pentacoordinate, spin-admixed systems characterized by a partially populated $d_{x^2-y^2}$ orbital, the Fe–N_p and $C_{t'}$···N distances have similar averages of 1.98 and 1.97 Å, respectively.[14,15,17,18] Also, an out-of-plane displacement of the iron atom (Fe···$C_{t'}$) in the range 0.10–0.33 Å is characteristic of low-spin or spin-admixed systems.[15,37] This raises the possibility that the spin-state composition of the iron(III) center in molecule **1** is varying with temperature.[22,25]

Table 9. Selected Intramolecular Bond Angles (deg) for $[Fe^{III}(TPP)(OSO_2CF_3)]$ at 293 K in the Triclinic Phase

O1–Fe1–N1	94.1(1)	O4–Fe2–N5	103.8(1)
O1–Fe1–N2	103.1(1)	O4–Fe2–N6	102.6(1)
O1–Fe1–N3	98.9(1)	O4–Fe2–N7	100.1(1)
O1–Fe1–N4	100.6(1)	O4–Fe2–N8	99.3(1)
N1–Fe1–N2	88.7(1)	N5–Fe2–N6	87.7(1)
N1–Fe1–N3	88.6(1)	N5–Fe2–N7	156.1(1)
N1–Fe1–N4	165.3(1)	N5–Fe2–N8	87.5(1)
N2–Fe1–N3	158.0(1)	N6–Fe2–N7	88.0(1)
N2–Fe1–N4	88.3(1)	N6–Fe2–N8	158.1(1)
N3–Fe1–N4	88.8(1)	N7–Fe2–N8	87.8(1)
O1–S1–O2	113.6(2)	O4–S2–O5	109.5(3)
O1–S1–O3	112.8(2)	O4–S2–O6	113.1(3)
O1–S1–C1S	101.7(3)	O4–S2–C2S	105.8(4)
O2–S1–O3	117.9(3)	O5–S2–O6	118.1(4)
O2–S1–C1S	104.2(3)	O5–S2–C2S	104.5(4)
O3–S1–C1S	104.3(3)	O6–S2–C2S	104.7(5)
Fe1–O1–S1	139.6(2)	Fe2–O4–S2	137.2(2)
S1–C1S–F1	112.1(5)	S2–C2S–F4	107.8(9)
S1–C1S–F2	112.3(5)	S2–C2S–F5	118.1(9)
S1–C1S–Fe	111.2(5)	S2–C2S–F6	113.4(7)
F1–C1S–F2	109.7(6)	F4–C2S–F5	103(1)
F1–C1S–F3	105.7(5)	F4–C2S–F6	104(1)
F2–C1S–F3	105.5(5)	F5–C2S–F6	110(1)

In an attempt to discover why molecules **1** and **2** display such different temperature dependencies, packing diagrams of the crystal structures have been examined. Since the geometry and orientation of axial ligands is known to cause variations in the iron spin state of porphyrin molecules,[47] the region around the axial $(SO_3CF_3)^-$ ligands was of particular interest. Specifically, it is instructive to compare the axial ligand's hydrogen-bonding interactions in this crystal system to those found in the monoclinic phase of $[Fe^{III}(TPP)(OSO_2CF_3)]$ as discussed above. The only unusual feature in this region appears to be a very close intermolecular contact distance between the F4 atom in the $(SO_3CF_3)^-$ ligand of molecule **2** with a hydrogen atom on a peripheral phenyl ring in a different molecule **2** in an adjacent unit cell. This F(4)···H–C distance is 2.3 Å in the 293 and 188 K structures and is well within the calculated distance of 2.6 Å for a C–H···F hydrogen bond.[48,49] All other intermolecular or intramolecular contacts appear to be at or in excess of the van der Waals radii of the atoms involved. It is possible that these close C–H···F interactions are influential enough to in some way "stabilize" the $S = {}^5/_2$ spin state contribution at all temperatures. No such interactions are present for molecule **1**. It is also noteworthy that the present $[Fe^{III}(TPP)(OSO_2CF_3)]$ structure is somewhat unusual for a metalloporphyrin in that it is devoid of solvent molecules of crystallization. The only other iron metalloporphyrin compound known to exhibit two distinct spin-

(45) The Fe–N_p and Fe···$C_{t'}$ distances of molecule **2** are 2.04(1) and 0.44(1) for the 103 K structure also indicating an $S = {}^5/_2$ Fe center. Poor data set quality makes bond distance comparisons between the 103 K structure and the other structures (and with others previously published) only *qualitative* at best, especially when comparing and assigning varying amounts of spin $S = {}^3/_2$ admixture. However, the same general conclusions are deduced by comparing the 293 and 188 K structures as by comparing the 293 and 103 K structures.

(46) The Fe–N_p distance for molecule **1** at 103 K is 1.98(1), and its Fe···$C_{t'}$ distance is 0.26 (1) Å.

(47) Geiger, D. K.; Lee, Y. J.; Scheidt, W. R. *J. Am. Chem. Soc.* **1984**, *106*, 6339.

(48) Hamilton, W. C.; Ibers, J. C. In *Hydrogen Bonding in Solids*; W. A. Benjamin: New York, 1968; p 16.

(49) Pimentel, G. C.; McClellan, A. L. In *The Hydrogen Bond*; W. H. Freeman: San Francisco, CA, 1960.

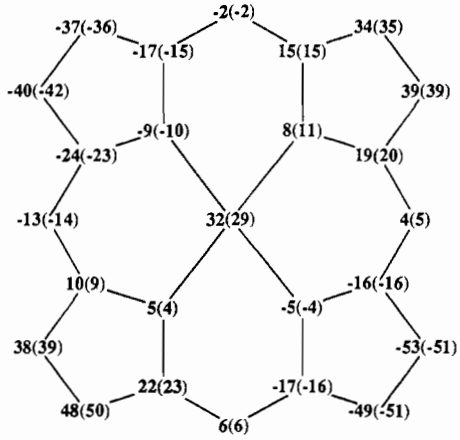

Figure 8. Formal diagram of the porphinato core of molecule **1** in [Fe^{III}(TPP)(OSO_2CF_3)] in the triclinic phase at 293 and 188 K (in parentheses) displaying the perpendicular displacements, in units of 0.01 Å, of each atom from the mean plane of the 24-atom core. The atom labels have been replaced by the value of the displacement.

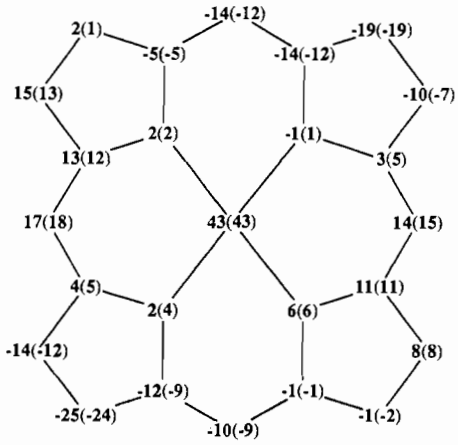

Figure 9. Formal diagram of the porphinato core of molecule **2** in [Fe^{III}(TPP)(OSO_2CF_3)] in the triclinic phase at 293 and 188 K (in parentheses) displaying the perpendicular displacements, in units of 0.01 Å, of each atom from the mean plane of the 24-atom core. The atom labels have been replaced by the value of the displacement.

state sites in the same crystal lattice is [Fe^{III}(TPP)(NCS)(Py)], which also crystallizes without molecules of solvation;[22] however, with a pyridine solvate molecule in the lattice, the same iron(III) complex possesses only $S = {}^1/_2$ sites.[50]

Formal diagrams of the porphinato skeleton in molecules **1** and **2** at 188 K are shown in Figures 8 and 9. The ruffling patterns of both molecules follow exactly the ones previously described (Sad for molecule **1** and Ruf for molecule **2**) in the room-temperature structure. The dihedral angles between the phenyl groups and the mean plane of the 24-atom porphyrin core are as follows: molecule **1**, 60.27, 86.84, 82.59, 47.54; molecule **2**, 65.03, 71.87, 83.62, 74.34°.

As expected, the previously noted phenomenon that molecule **1** is involved in a strong $\pi-\pi$ dimer interaction while molecule **2** is not is also found in the low-temperature structure. ORTEP representations of edge-on views (molecules **1** and **2**) and models representing the strong overlap of the two porphyrin cores (molecules **1** and **2**) are available as supplementary material. Table 12 shows a comparison of all the dimer interaction parameters for both molecules at both temperatures. A few important points can be made about the data in this table. First, the lateral shift (LS) and the distance between the centers of the porphyrin macrocycle (C_t···$C_{t'}$), which are combinations of the

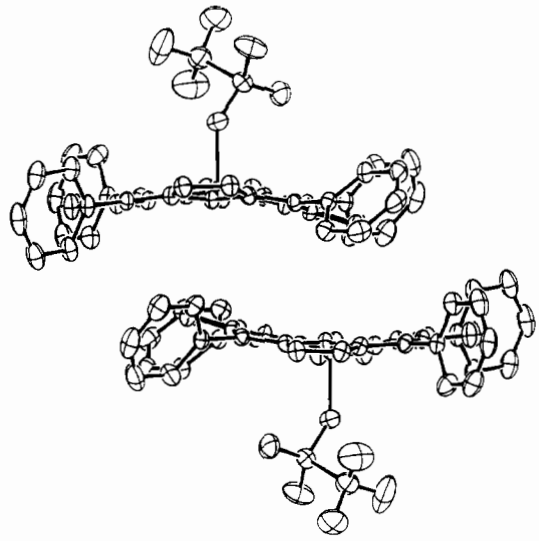

Figure 10. Edge-on view of a molecule **1** dimer in [Fe^{III}(TPP)(OSO_2CF_3)] at 293 K in the triclinic phase.

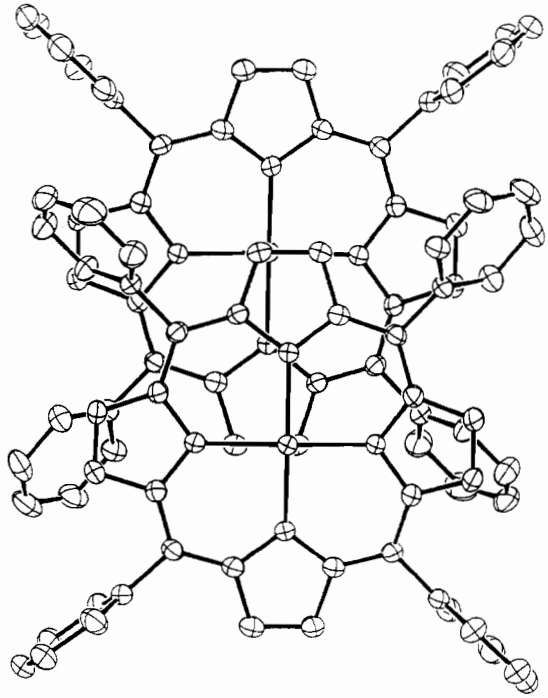

Figure 11. Projection of the two porphyrin planes within a dimer of molecule **1** in [Fe^{III}(TPP)(OSO_2CF_3)] at 293 K in the triclinic phase.

other parameters, remain essentially unchanged with temperature within a given molecule. Also, these distances are about 1 Å longer at all temperatures in the "noninteracting" molecule **2**. These values, along with the core overlap characteristics in both molecules, indicate that molecule **1** interacts in the solid state by forming type I $\pi-\pi$ dimers[37] at both temperatures, while molecule **2** does not. Finally, the variation with temperature in Fe···Fe distances should be noted. As it can be seen in Table 12, the Fe2···Fe2 distance remains fairly constant in both structures. However, the Fe1···Fe1 distance decreases considerably from 5.718(2) Å at 293 K to 5.602(4) Å at 188 K.[51] This observation supports the possibility that, as temperature is decreased, the amount of $S = {}^3/_2$ character in the spin-state composition of the iron(III) center in molecule **1** is increasing therefore causing the iron atom to move more "in-plane" with the porphinato core,[14,15,17,18] thus shortening the Fe1···Fe1 separation. It is still

(50) Scheidt, W. R.; Lee, Y. J.; Geiger, D. K.; Taylor, K.; Hatano, K. *J. Am. Chem. Soc.* **1982**, *104*, 3367.

(51) For the 103 K structure, Fe1···Fe1 is 5.535(5) Å and Fe2···Fe2 is 6.989-(6).

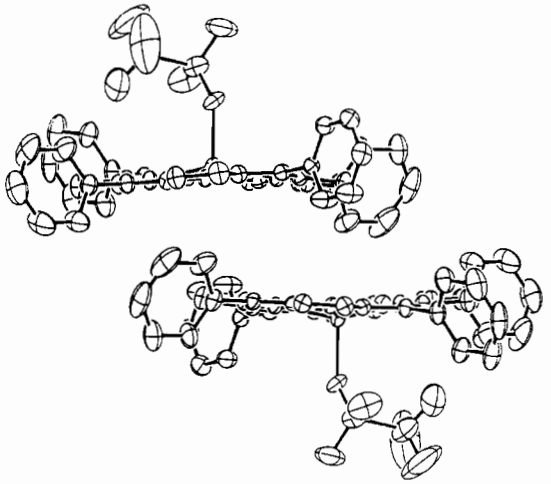

Figure 12. Edge-on view of a molecule **2** dimer in [Fe^{III}(TPP)(OSO_2CF_3)] at 293 K in the triclinic phase.

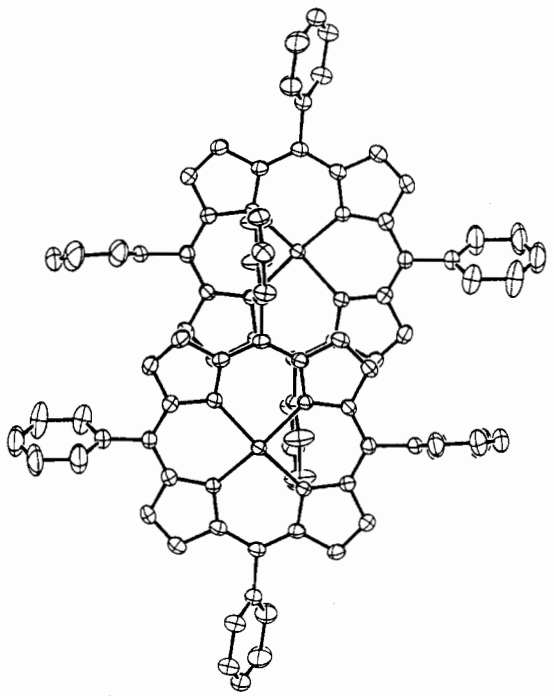

Figure 13. Projection of the two porphyrin planes within a dimer of molecule **2** in [Fe^{III}(TPP)(OSO_2CF_3)] at 293 K in the triclinic phase.

Table 10. Selected Intramolecular Distances (Å) for [Fe^{III}(TPP)(OSO_2CF_3)] at 188 K in the Triclinic Phase

Fe1–O1	1.996(6)	Fe2–O4	1.982(7)
Fe1–N1	1.972(8)	Fe2–N5	2.036(7)
Fe1–N2	2.013(7)	Fe2–N6	2.019(8)
Fe1–N3	2.011(7)	Fe2–N7	2.039(8)
Fe1–N4	1.979(8)	Fe2–N8	2.052(8)
S1–O1	1.447(6)	S2–O4	1.392(7)
S1–O2	1.427(7)	S2–O5	1.441(8)
S1–O3	1.418(8)	S2–O6	1.449(9)
S1–C1S	1.81(1)	S2–C2S	1.85(2)
C1S–F1	1.30(1)	C2S–F4	1.35(2)
C1S–F2	1.32(1)	C2S–F5	1.18(2)
C1S–F3	1.32(1)	C2S–F6	1.31(2)

an open question whether π–π dimer interactions can influence the geometrical environment around the metal center in porphyrin derivatives.[37,52] While the above structural data alone are inconclusive in establishing a variation in the Fe–N_p bond distances with temperature (3σ criterion), the statistically significant change

Table 11. Selected Intramolecular Bond Angles (deg) for [Fe^{III}(TPP)(OSO_2CF_3)] at 188 K in the Triclinic Phase

O1–Fe1–N1	93.1(3)	O4–Fe2–N6	103.7(3)
O1–Fe1–N2	103.0(3)	O4–Fe2–N7	100.7(3)
O1–Fe1–N3	98.0(3)	O4–Fe2–N8	98.4(3)
O1–Fe1–N4	99.8(3)	N5–Fe2–N6	87.7(3)
N1–Fe1–N2	88.9(3)	N5–Fe2–N7	156.6(3)
N1–Fe1–N3	88.9(3)	N5–Fe2–N8	87.0(3)
N1–Fe1–N4	167.1(3)	N6–Fe2–N7	88.0(3)
N2–Fe1–N3	159.0(3)	N6–Fe2–N8	157.8(3)
N2–Fe1–N4	88.5(3)	N7–Fe2–N8	88.3(3)
N3–Fe1–N4	88.9(3)	O4–S2–O5	110.5(5)
O1–S1–O2	113.3(4)	O4–S2–O6	114.4(5)
O1–S1–O3	114.0(4)	O4–S2–C2S	102.6(8)
O1–S1–C1S	101.2(5)	O5–S2–O6	117.4(6)
O2–S1–O3	118.0(5)	O5–S2–C2S	103.5(7)
O2–S1–C1S	103.0(5)	O6–S2–C2S	106.6(9)
O3–S1–C1S	104.6(6)	Fe2–O4–S2	135.8(4)
Fe1–O1–S1	138.9(4)	S2–C2S–F4	106(2)
S1–C1S–F1	112.6(9)	S2–C2S–F5	117(2)
S1–C1S–F2	110.5(9)	F2–C1S–F3	105(1)
S1–C1S–F3	110.9(9)	S2–C2S–F6	110(1)
F1–C1S–F2	109(1)	CF4–C2S–F5	110(2)
F1–C1S–F3	108(1)	F4–C2S–F6	100(2)
O4–Fe2–N5	102.7(3)	F5–C2S–F6	112(2)

Table 12. Dimer Interaction Parameters for Molecule **1** and Molecule **2** in [Fe^{III}(TPP)(OSO_2CF_3)] in the Triclinic Phase at 293 and 188 K[a]

T (K)	Fe···Fe	LS	C_t···$C_{t'}$	MPS	SA (deg)
		Molecule **1**			
293	5.718(2)	3.01	4.86	3.82	38.23
188	5.602(4)	3.04	4.83	3.75	39.02
		Molecule **2**			
293	6.997(2)	4.14	5.73	3.96	46.28
188	6.943(5)	4.11	5.65	3.88	46.67

[a] All distances are given in Å; standard deviations are shown in parentheses.

in the Fe1···Fe1 distance with temperature, as well as the multiple temperature magnetic and spectroscopy data (see below), together strongly indicate that the spin state of molecule **1** is indeed temperature dependent.

Magnetic Properties and Mössbauer and EPR Spectroscopy Results. The variable-temperature magnetic susceptibility data in Figure 1 displays non-Curie behavior for [Fe^{III}(TPP)(OSO_2CF_3)]. For other spin-admixed systems, the Maltempo model[10,13] (or variations thereof) has been employed to analyze variable-temperature magnetic data. In these cases, limiting values of $<5.0\ \mu_B$ at room temperature for solid samples have been characteristic of the admixed ground state. For [Fe^{III}(TPP)(OSO_2CF_3)] a value of $5.8\ \mu_B$ at 293 K, therefore, suggests a large contribution of the $S = {}^5/_2$ spin state for this compound, and this is reflected in the 293 K crystal structure for both the monoclinic and triclinic crystal systems. We have chosen not to attempt a Maltempo analysis for the present polycrystalline sample because (1) the above structural results (and the spectroscopic data presented below) indicate a three-component spin system, (2) the spin-state composition of one of the admixed sites (triclinic, molecule **1**) may not be temperature independent, (3) there is a lack of magnetic data below 20 K where Fe···Fe magnetic interactions become most evident [40,42,53] and where variation in the magnetic susceptibility arising from Maltempo behavior is most prominent, and finally (4) a large percentage of the iron(III) centers in bulk [Fe^{III}(TPP)(OSO_2CF_3)] are strongly interacting via π–π dimer formation (molecule **1**, triclinic phase) while the remaining centers (molecule **2** in the triclinic phase and all molecules in the monoclinic phase) are not.

Compelling evidence for the assignment of two magnetically distinct lattice sites for triclinic [Fe^{III}(TPP)(OSO_2CF_3)] also

(52) Kutzler, F. W.; Swepston, P. N.; Berkovitch-Yellin, Z.; Ellis, D. E.; Ibers, J. A. *J. Am. Chem. Soc.* **1983**, *105*, 2996.

(53) Gupta, G. P.; Lang, G.; Scheidt, W. R.; Geiger, D. K.; Reed, C. A. *J. Chem. Phys.* **1985**, *83*, 5945.

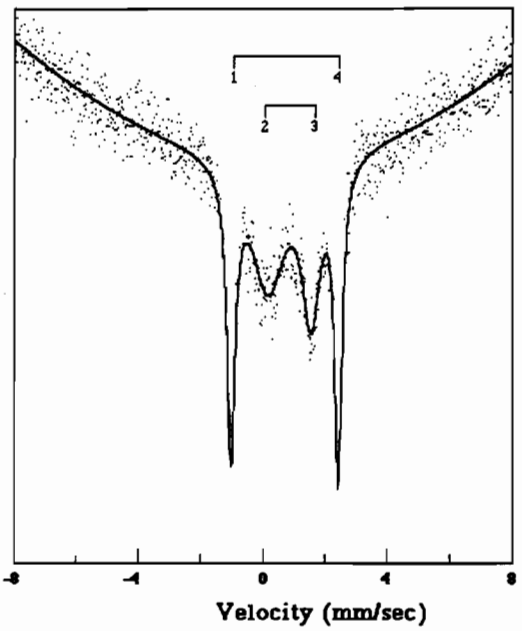

Figure 14. Mössbauer spectrum of $[Fe^{III}(TPP)(OSO_2CF_3)]$ at 6 K. Signals 1 and 4: doublet from molecule **1**, triclinic phase. Signals 2 and 3: doublet from monoclinic phase and molecule **2**, triclinic phase. The solid line is a least-squares fit.

comes from the Mössbauer spectra displayed in Figure 14. The spectral parameters obtained at 6, 77, and 150 K are listed in Table 13, along with comparative literature values for other high-spin and spin-admixed systems with varying amounts of $S = {}^3/_2$ character. In the absence of an applied magnetic field, the spectrum of $[Fe^{III}(TPP)(OSO_2CF_3)]$ shows two sharp and well-defined quadrupole split doublets at all temperatures. Large quadrupole splittings are characteristic of intermediate spin states ($S = {}^3/_2$),[14,18,56] and therefore, the larger quadrupole-split doublet (signals 1 and 4) in Figure 14 is assigned to molecule **1** (triclinic), while the smaller quadrupole-split doublet (signals 2 and 3) is assigned to molecules in the monoclinic lattice plus molecule **2** of the triclinic phase. Presumably, the combination of these two nearly $S = {}^5/_2$ species is the reason for the particular broadness of this doublet. The isomer shift values obtained for both quadrupole-split doublets are in the range expected for iron in the +3 oxidation state.[13,14,18] Also, the values for ΔE_Q obtained for the outer and inner doublets compare favorably with other values which have been reported for intermediate spin-admixed and mainly high-spin systems, respectively. On the basis of a ΔE_Q value for the inner doublet of 1.45 mm/s, it is believed that the iron(III) ground state for molecule **2** and the molecules of the monoclinic phase contains only a small amount of $S = {}^3/_2$ character.

The Mössbauer spectrum at 6 K shows molecule **1** with ~75% $S = {}^3/_2$ character when its ΔE_Q and structural parameters are compared to those of other similar species (see Tables 7 and 13). The spectra obtained at the three different temperatures are identical in shape with the sum of the integrated areas under signals 1 and 4 remaining fairly constant relative to the sum of the areas under signals 2 and 3 (approximately 40:60 integrations). This interpretation also explains the plateau in the 20–80 K region of the μ_{eff} data in Figure 1; in this temperature regime, molecule **1** has largely completed its molecular transformation and its structure is essentially constant by 80 K. From 100 to 300 K, molecule **1** seems to obtain more $S = {}^5/_2$ character until it is ~30% $S = {}^5/_2$ at room temperature (from comparing its structural parameters to those of $[Fe^{III}(TPP)(OSO_2CF_3)]$ in the monoclinic phase and from the EPR data below) where molecule **2** is also essentially only $S = {}^5/_2$. This can also be seen in the Mössbauer spectral parameters obtained at 150 K where ΔE_Q for molecule **1** continues to collapse toward a value characteristic of more $S = {}^5/_2$ character, while that for molecule **2** remains essentially unchanged. It should be noted that temperature-dependent quadrupole splittings (2.8 mm/s $\leq \Delta E_Q \leq$ 3.5 mm/s) have been previously observed for several (but not all) spin-admixed iron(III) porphyrins.[57] The reason for this behavior is not well understood, but a spin-state with a "dynamic" admixture has been postulated as a possible explanation.[57] Moreover, none of the other intermediate admixed-spin compounds which are known to exhibit this Mössbauer behavior have been subjected to a variable-temperature X-ray structure determination such as the one presented here. We, therefore, suggest that the large temperature-dependent ΔE_Q values observed for $[Fe^{III}(TPP)(OSO_2CF_3)]$ possibly arise from an admixed ground state of iron(III) in thermal equilibrium with a slightly different admixed excited state within $\sim kT$ of the ground state. This would be a spin-equilibrium for admixed iron(III), and for an averaged Mössbauer spectrum of the two spin states to be observed (as is the case here), the rate of spin-state interconversion would need to exceed the 10^7 s^{-1} spectral time scale. This situation has been previously observed for other porphyrin iron(III) spin-equilibrium species studied by Mössbauer spectroscopy.[23,58–60] Interestingly, similar Mössbauer behavior is exhibited by a binuclear [Fe(III)porphyrin–Cu(II)] complex reported by Buckingham *et al.*[61] In this work, two Mössbauer doublets which feature temperature-dependent quadrupole splittings were interpreted to indicate some form of spin-equilibrium situation where the contributions from high-spin ($S = {}^5/_2$) and admixed-spin ($S = {}^5/_2, {}^3/_2$) iron(III) centers varied with temperature, possibly causing structural alterations as the temperature was changed.[61]

As a final comment, it is important to point out that whether an admixed–spin compound exhibits a temperature dependent ΔE_Q is not contingent upon it interacting via π–π dimer formation in the solid state (see Table 13). This is evidenced by the fact that while $[Fe^{III}(OEP)(OClO_3)]$, a type I π–π dimer,[37] displays a temperature-dependent ΔE_Q (3.57 mm/s at 4.2 K decreasing to 3.16 mm/s at 295 K),[56,57] $[Fe^{III}(TPP)(HB_{11}CH_{11})]$ (ΔE_Q = 4.12 mm/s)[18] and $[Fe^{III}(OEP)(3\text{-}Clpy)]ClO_4$ (ΔE_Q = 3.23 mm/s)[15] do not.

A low-temperature (11 K) EPR spectrum collected on a polycrystalline sample of $[Fe^{III}(TPP)(OSO_2CF_3)]$ is shown in Figure 15 to display three expectedly broad signals at $g_\perp \sim 6.01$, 5.52 and at $g_\parallel \sim 2.12$. In general, an axial EPR spectrum with a $6 > g_\perp > 4$ range is the normal signature of an $S = {}^5/_2, {}^3/_2$ admixed-spin state for iron(III) porphyrins, with $g_\perp$ linearly related to the percentage of $S = {}^3/_2$ in the admixed state with boundary values from 0% ($g_\perp \sim 6$) to 100% ($g_\perp \sim 4$). On the other hand, a $g_\perp = 6$ signal is indicative of an $S = {}^5/_2$ state. Thus, the signal at $g_\perp = 6.01$ (~0% $S = {}^3/_2$) can be assigned to molecule **2** present in the triclinic lattice, while the signal at $g_\perp = 5.52$ (~25% $S = {}^3/_2$) can be attributed to the molecules present in the monoclinic lattice. To conclude the analysis of the EPR spectrum, it should be again noted that no signal is necessarily expected for molecule **1** of the triclinic lattice because these molecules form π–π dimers of the nature that they are likely to be EPR silent through coupled spin-pairs of the dimers.[15,18,40] If

(54) Moy, S. A. Ph.D. Dissertation, Chemistry Department, Rice University, Houston, TX, 1990.
(55) Wilson, L. J.; Moy, S. A.; Gonzalez, J. A. *Acta Crystallogr.*, in press.
(56) Dolphin, D. H.; Sams, J. R.; Tsin, T. B. *Inorg. Chem.* **1977**, *16*, 711.
(57) Debrunner, P. G. In *Physical Bioinorganic Chemistry-Iron Porphyrins, Part III*; Lever, A. B. P., Gray, H. B., Eds.; VCH Publishers, Inc.: New York, 1989; pp 137–227.
(58) Scheidt, W. R.; Geiger, D. K.; Haller, K. J. *J. Am. Chem. Soc.* **1982**, *104*, 495.
(59) Malliaris, A.; Papaefthimiou, V. *Inorg. Chem.* **1982**, *21*, 770.
(60) Merithew, P. B.; Rasmussen, P. G. *Inorg. Chem.* **1972**, *11*, 325.
(61) Gunter, M. J.; Mander, L. N.; McLaughlin, G. M.; Murray, K. S.; Berry, K. J.; Clark, P. E.; Buckingham, D. A. *J. Am. Chem. Soc.* **1980**, *102*, 1470.

Table 13. Mössbauer Parameters for [Fe^{III}(TPP)(OSO_2CF_3)] and Comparisons with Other Representative Complexes

complex	T (K)	% $S = {}^3/_2$[a]	δ[b]	ΔE_Q[c]	ΔE_Q temp dependent	π–π dimers	ref
[Fe(TPP)($OCOCF_3$)]	77	0	0.42	0.79	no	no	54, 55
[Fe(OEP)(2-MeHIm)]ClO_4	4	2	0.40	1.39	n.a.	yes	18, 43
[Fe(TPP)(OSO_2CF_3)] monoclinic and	150	*d*	0.49	1.40	yes	no	this work
molecule **2** (triclinic)	77	*d*	0.36	1.50	yes	no	this work
	6	*d*	0.59	1.46	yes	no	this work
[Fe(TPP)(OSO_2CF_3)] molecule **1** (triclinic)	150		0.40	2.79	yes	yes	this work
	77		0.31	3.07	yes	yes	this work
	6		0.44	3.56	yes	yes	this work
[Fe(TPP)($OClO_3$)]	4	65	0.38	3.48	yes	no	14
[Fe(OEP)($OClO_3$)]	4	80	0.37	3.57	yes	yes	56, 57
[Fe(OEP)(3-Clpy)]ClO_4	4	81	0.36	3.23	no	yes	15, 40
[Fe(TPP)($HB_{11}CH_{11}$)]	4	92	0.33	4.12	no	yes	18
[Fe(TPP)($FSbF_5$)]	4	98	0.39	4.29	no	no	17

[a] These values are obtained from $g_\perp$ when the compound is EPR active and from magnetic susceptibility and high field Mössbauer spectroscopy when π–π dimers make the compound EPR silent. [b] In mm/s. Given relative to metallic iron ($\delta_{SNP} = \delta_{Fe} + 0.26$). [c] In mm/s. Estimated error: 0.05 mm/s. [d] $S = {}^3/_2$ character for [Fe(TPP)(OSO_2CF_3)] in the monoclinic phase is ~25%. $S = {}^3/_2$ character for molecule **2** of [Fe(TPP)(OSO_2CF_3)] in the triclinic phase is ~0%. See discussion in text.

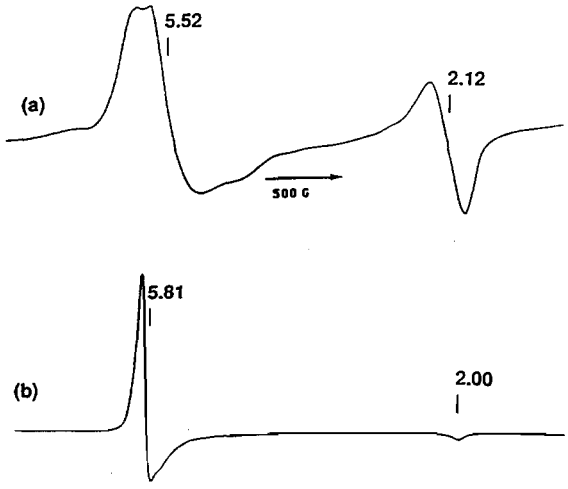

Figure 15. EPR spectrum at 11 K for [Fe^{III}(TPP)(OSO_2CF_3)]: (a) in the polycrystalline state; (b) in a toluene glass.

the EPR signal were not quenched by this mechanism, a signal of $g \sim 4$ at 11 K for molecule **1** might be anticipated because the low-temperature X-ray structure already indicates a significant amount of % $S = {}^3/_2$ character by 188 K.

Anisotropy effects are the probable cause of the unusually strong, broad axial $g_\parallel = 2.12$ signal in the spectrum. In this respect, the shape of the spectrum in Figure 15a displays a remarkable resemblance to that for Japanese radish peroxidase (pH 3.9) which may posses a heterogenous mixture of spin-admixed iron(III) centers.[13] In frozen solution (Figure 15b), all evidence of molecular heterogeneity for [Fe^{III}(TPP)(OSO_2CF_3)] disappears and a single, axial $g \sim 5.8$, 2.0 signal is obtained, indicating that all the molecules become electronically equivalent in solution.

Conclusions

[Fe^{III}(TPP)(OSO_2CF_3)] in both a monoclinic and triclinic phase is structurally and spectroscopically characterized here for the first time. In the monoclinic phase, the compound exhibits typical characteristics of an spin-admixed iron(III) porphyrin compound with a considerable amount of $S = {}^5/_2$ character in the ground state. [Fe^{III}(TPP)(OSO_2CF_3)] in the triclinic phase is the first pentacoordinate [Fe^{III}(Por)X] system to exhibit spin-state isomerism in the solid state with two crystallographically and magnetically distinct sites in the same unit cell. One of the sites is unique in being possibly the first reported case of a structurally-characterized "dynamic" spin-admixed center undergoing a spin-equilibrium which is fast on the Mössbauer time scale. The second spin-admixed site exhibits mainly temperature-independent high-spin characteristics. This triclinic phase is also the first iron porphyrin system reported in which molecule pairs in the same unit cell interact in a markedly different fashion with one dimer pair exhibiting a strong π–π interaction while the second pair does not.

Acknowledgment. This work was supported by National Institutes of Health Grant GM-28451 from the National Institute of General Medical Sciences and Grant C-624 from the Robert A. Welch foundation. The Rigaku AFC-5S X-ray diffractometer was purchased, in part, through an instrumentation grant from the National Science Foundation. We thank Daniel W. Lee for obtaining the magnetic susceptibility data and Dr. Shirley A. Moy for the Mössbauer data. We also thank Dr. Joe Ferrara for helpful discussions concerning the refinement of the crystal structures.

Supplementary Material Available: Tables giving crystal data and details of the structure determination, atom coordinates, bond lengths, bond angles, anisotropic thermal parameters, hydrogen atom locations, and rigid group derived coordinates for the three crystal structures and figures for [Fe^{III}(TPP)(OSO_2CF_3)] in the triclinic phase at 188 K including ORTEP plots of molecules **1** and **2**, ORTEP representations of edge-on views (molecules **1** and **2**), and models representing the overlap of the two porphyrin cores (molecules **1** and **2**) (59 pages). Ordering information is given on any current masthead page.